NOTES AND CORRESPONDENCE

Evidence of Saturation in a Gravity-Wave Critical Layer

TIMOTHY J. DUNKERTON AND ROBERT E. ROBINS

Northwest Research Associates, Bellevue, Washington

3 July 1991 and 25 February 1992

1. Introduction

In a companion paper, we described the transition from laminar flow to convective turbulence in two-dimensional numerical simulations of a gravity-wave critical layer (Dunkerton and Robins 1992, hereafter DR). Vertical velocity spectra revealed a high-wavenumber continuum of nonradiating convective instability within the region of isentropic overturning, together with a new "radiating" mode of secondary instability centered in the overturned region, but also having significant amplitude in adjacent stable regions of the wave field. Surprisingly, the radiating mode developed prior to nonradiating convection and displayed scale selection, unlike nonradiating instability with its grid-dependent zonal wavelength. Dunkerton and Robins showed that radiating instability was an unstable eigenmode in a parallel-flow approximation.

As a follow-up to that study, we describe in this note the results of nonlinear, nonhydrostatic integrations well beyond the time of initial overturning. Regular "cellular" structure of secondary instability has then given way to chaotic, small-scale features. In inviscid simulations, the cascade to small scales generally leads to numerical instability; it can be kept under control with scale-dependent damping (DR). This procedure allows long-time numerical simulation of gravity waves coexisting with "turbulence." With judicious choice of damping, it is possible to simulate primary wave and secondary instability as though the flow were inviscid; only smaller-scale turbulence resulting from secondary instability is damped. Equilibration occurs as the primary wave supplies energy to instabilities, which feed smaller-scale motions, which are, in turn, selectively removed by damping.

Although there is an initial time lag between overturning and outbreak of instability, turbulence develops rapidly thereafter and effectively "saturates" the primary wave. The effect is that wave amplitude cannot greatly exceed its marginally unstable value—the same threshold assumed in convective saturation theory (Lindzen 1981; Dunkerton 1982; Holton 1983; Fritts 1984; Lindzen 1988; Schoeberl 1988; Dunkerton 1989).

We believe it is worthwhile to demonstrate the equilibration with direct numerical simulation, and to do so in a configuration where primary wave forcing is held constant at the lower boundary. In a slightly different context, Bacmeister and Schoeberl (1989) observed breakdown of orographic waves, which had the effect of altering the wave forcing, leading to an oscillatory kind of "equilibration." This behavior may be important whenever gravity wave breaking interacts with the region of excitation. On the other hand, it is interesting to consider what happens when wave breaking is kept isolated from the source, as presumably occurs in nonorographic situations. In any event, this case corresponds more closely to saturation theory cited above.

2. Results

a. Nonhydrostatic numerical model

The numerical model used here was a nonlinear, time-dependent version of the linear nonhydrostatic code used by DR to study temporal development of secondary instabilities on a fixed basic state. As such, it was identical to Dunkerton's (1987) model except that horizontal resolution was increased and evaluation of nonlinear Jacobians done with an FFT to physical space.

For simulation, 128 zonal harmonics and 201 vertical grid points were used in a domain 50 km wide and 10 km deep (as in DR). The same forcing of stationary vertical velocity perturbation at the lower boundary was used as in DR. The initial mean flow had linear shear with a critical level at 8-km altitude. Two simulations are reported here, with identical parameters; in the second simulation, the mean-flow modification was included. Mean-flow evolution and the structure of secondary instability in this simulation were illustrated in the Appendix of DR.

Scale-dependent damping was second-order diffu-

Corresponding author address: Dr. Timothy J. Dunkerton, Northwest Research Associates, P.O. Box 3027, Bellevue, WA 98009.

sion (128 $m^2 s^{-1}$) modulated by a hyperbolic tangent function centered on zonal wavenumber $k = 60$ having width $\Delta k = 4$. The damping was nearly zero below zonal wavenumber 48 and close to the maximum for wavenumbers above 72.

b. *Secondary instability*

Initial evolution of the primary wave up to the point of overturning was virtually identical to the linear simulation reported in DR. The radiating mode of secondary instability was also similar (not shown). It was associated with a spectral peak near zonal wavenumbers 40–48, as shown in Fig. 1. The spectrum indicated a "doubling" effect with second peak around wavenumber 84 as noted by DR in a hydrostatic simulation. Doubling was visible only when the convection continuum was suppressed by scale-dependent damping.

Zonal wavenumber of radiating instability was somewhat higher than observed in a linear run with fixed basic state (DR); this is because DR's linear run began arbitrarily at 24 000 sec whereas the instability developed sooner in the nonlinear run, becoming visible near 21 000 sec (Fig. 1). During this time, the primary wave changed slightly, altering the wavenumber of the most unstable eigenmode. The position of the spectral peak in Fig. 1 was apparently determined by the structure of primary wave at 17 000–20 000 sec.

c. *Saturation and equilibration of primary wave*

Figure 2 shows potential temperature at 30 000 sec. By this time, the vertical velocity spectrum had equilibrated to its final shape (Fig. 1). The top panel shows the total field (all zonal wavenumbers) and the bottom panel shows a low-pass–filtered version (zonal wavenumbers 1–3 only). We note that while the finestructure in Fig. 2a changed continually with time, the low-pass field remained essentially the same throughout the remainder of the simulation (from 30 000 to 50 000+ s). Low-pass–filtered potential temperature contours overturned from time to time, but did not remain overturned; on average, they were neutral to convection, and hence suggest a "saturation" of the primary wave. In fact, the low-wavenumber flow did not differ much from low-resolution simulations with convective adjustment (see Dunkerton and Fritts 1984).

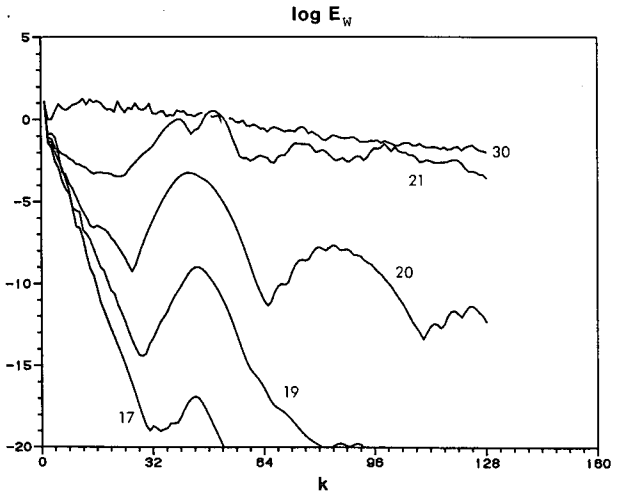

FIG. 1. Zonal wavenumber spectrum of vertical velocity squared, integrated over the model domain, in experiment with mean flow held constant. Labels denote time in seconds × 1000.

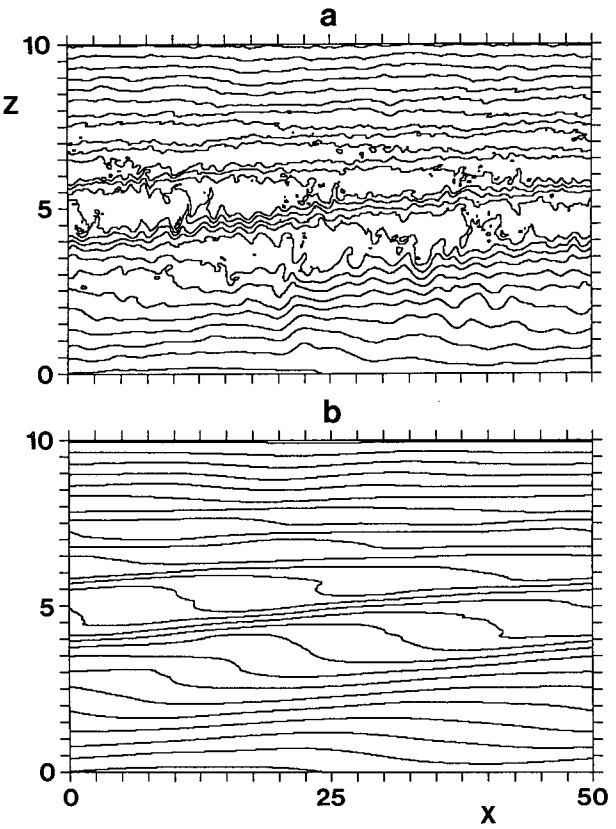

FIG. 2. (a) Potential temperature at 30 000 sec (all zonal wavenumbers); (b) Low-pass–filtered potential temperature at 30 000 sec (wavenumbers 1–3 only). Units on axes: kilometers.

There was some evidence of critical layer "transmission" in low- and high-wavenumber components (Figs. 2a and 2b) although the effect was rather small. Dunkerton (1987) observed a small amount of transmission due to resonant interaction. Here, it is more likely that transmitted components were generated in the turbulent critical layer and were therefore mostly nonresonant.

d. *Comparison of hydrostatic and nonhydrostatic models*

Comparing these results with DR, the hydrostatic approximation was valid for the primary wave and

(qualitatively, at least) secondary instability also. There was, however, an essential difference between the two models after overturning and development of critical-layer turbulence. This could be seen in the amount of *downward-propagating secondary wave activity* below the critical layer.

The nonhydrostatic model required that intrinsic frequency not exceed the Brunt–Väisälä frequency for vertical propagation. Consequently, downward propagation at high zonal wavenumber was prevented. Such disturbances were instead evanescent.

The hydrostatic model had no such requirement. As a result, the convection continuum not only dominated the critical layer, but launched narrow waves propagating down to the model lower boundary! In this sense, the critical layer simulation with hydrostatic code was not only unrealistic, but numerically ill behaved. (We caution against the use of hydrostatic models in this context unless care is taken to prevent spurious wave propagation.)

e. *Results with mean-flow modification*

The same experiment was done with mean-flow modification due to gravity-wave momentum flux convergence (as described in the Appendix of DR). Potential temperature at 30 000 sec is shown in Figs. 3a and 3b (with and without low-pass filter). Most of the domain was involved in wave breaking, but the same kind of saturation and equilibration could be seen in low-pass data (Fig. 3b; cf. Fig. 2b). Perhaps because of wave breaking near the lower boundary, the simulation had to be terminated not long after this time. Nevertheless, it seems that saturation was effective throughout the final ~9000 seconds of integration. Again, some evidence of transmission could be seen.

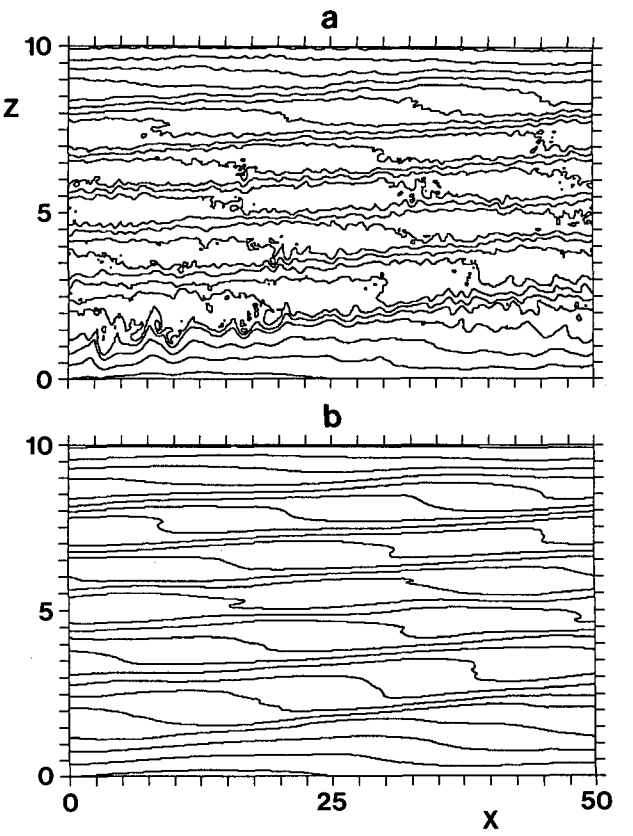

FIG. 3. Potential temperature at 30 000 sec as in Fig. 2, but for experiment with mean-flow modification. (a) All zonal wavenumbers; (b) wavenumbers 1–3 only.

3. Conclusions

Numerical simulations of a gravity-wave critical layer demonstrated a "saturated" equilibration between lower boundary forcing, generation of turbulence in the critical layer, and scale-dependent damping at the high end of the zonal wavenumber spectrum. Results suggest that convective adjustment becomes effective soon after onset of isentropic overturning. Immediately after overturning, secondary instabilities develop (DR), but give way to chaotic, small-scale features. Mean-flow modification alters the location and structure, but not the existence, of secondary instability and saturation.

We note that several types of secondary instability are possible, depending on initial flow configuration (mean flow plus primary wave). Strong mean shear, for example, could lead to Kelvin–Helmholtz instability in the wave field rather than convective instability. Furthermore, although the secondary instability did not significantly affect mean-flow evolution in cases reported here, one can imagine otherwise. An example would be the reduction or reversal of momentum flux below the critical layer due to radiating secondary instability.

These results qualitatively support convective saturation theory, but suggest that the problem be investigated further with other kinds of mean-flow profiles and wave parameters before drawing general conclusions.

It is interesting to speculate how the results would generalize to three-dimensional flow. To the extent that 3D turbulence is more vigorous—specifically, more efficient in the downgradient transport of heat—it is reasonable to expect that (someday) saturation will be demonstrated in three-dimensional numerical simulations.

Acknowledgments. This research was supported by the Air Force Office of Scientific Research, Contract F49620-89-C-0051, and by the National Science Foundation, Grant ATM-8819582. Partial computing support was also provided by the National Center for

Atmospheric Research, which is sponsored by the National Science Foundation.

REFERENCES

Bacmeister, J. T., and M. R. Schoeberl, 1989: Breakdown of vertically propagating two-dimensional gravity waves forced by orography. *J. Atmos. Sci.*, **46,** 2109–2134.

Delisi, D. P., and T. J. Dunkerton, 1989: Laboratory observations of gravity wave critical-layer flows. *Pure Appl. Geophys.*, **130,** 445–461.

Dunkerton, T. J., 1982: Wave transience in a compressible atmosphere, Part 3: The saturation of internal gravity waves in the mesosphere. *J. Atmos. Sci.*, **39,** 1042–1051.

——, 1987: Effect of nonlinear instability on gravity wave momentum transport. *J. Atmos. Sci.*, **44,** 3188–3209.

——, 1989: Theory of internal gravity wave saturation. *Pure Appl. Geophys.*, **130,** 373–397.

——, and D. C. Fritts, 1984: The transient gravity wave critical layer, Part I: Convective adjustment and the mean zonal acceleration. *J. Atmos. Sci.*, **41,** 992–1007.

——, and R. E. Robins, 1992: Radiating and nonradiating modes of secondary instability in a gravity-wave critical layer. *J. Atmos. Sci.*, **49,** 2546–2559.

Fritts, D. C., 1984: Gravity wave saturation in the middle atmosphere: A review of theory and observations. *Rev. Geophys. Space Phys.*, **22,** 275–308.

Holton, J. R., 1983: The influence of gravity wavebreaking on the general circulation of the middle atmosphere. *J. Atmos. Sci.*, **40,** 2497–2507.

Lindzen, R. S., 1981: Turbulence and stress due to gravity wave and tidal breakdown. *J. Geophys. Res.*, **86C,** 9707–9714.

——, 1988: Supersaturation of vertically propagating internal gravity waves. *J. Atmos. Sci.*, **45,** 705–711.

Schoeberl, M. R., 1988: A model of stationary gravity wave breakdown with convective adjustment. *J. Atmos. Sci.*, **45,** 980–992.